J Mater Sci: Mater Med (2006) 17:647–657
DOI 10.1007/s10856-006-9228-4

Development of an optimized electrochemical process for subsequent coating of 316 stainless steel for stent applications

M. Haïdopoulos · S. Turgeon · C. Sarra-Bournet · G. Laroche · D. Mantovani

Received: 19 January 2004 / Accepted: 24 October 2005

Abstract Metallic endovascular stents are used as medical devices to scaffold biological lumen, most often diseased arteries, after balloon angioplasty. They are commonly made of 316L stainless steel or Nitinol, two alloys containing nickel, an element classified as potentially toxic and carcinogenic by the International Agency for Research on Cancer. Although they are largely implanted, the long-term safety of such metallic elements is still controversial, since the corrosion processes may lead to the release of several metallic ions, including nickel ions in diverse oxidation states. To avoid metallic ion release in the body, the strategy behind this work was to develop a process aiming the complete isolation of the stainless steel device from the body fluids by a thin, cohesive and strongly adherent coating of RF-plasma-polymerized fluoropolymer. Nevertheless, prior to the polymer film deposition, an essential aspect was the development of a pre-treatment for the metallic substrate, based on the electrochemical polishing process, aiming the removal of any fragile interlayer, including the native oxide layer and the carbon contaminated layer, in order to obtain a smooth, defect-free surface to optimize the adhesion of the plasma-deposited thin film. In this work, the optimized parameters for electropolishing, such as the duration and the temperature of the electrolysis, and the complementary acid dipping were presented and accurately discussed. Their effects on roughness as well as on the evolution of surface topography were investigated by Atomic Force Microscopy, stylus profilometry and Scanning Electron Microscopy. The modifications induced on the surface atomic concentrations were studied by X-ray Photoelectron Spectroscopy. The improvements in terms of the surface morphology after the pre-treatment were also emphasized, as well as the influence of the original stainless steel surface finish.

M. Haïdopoulos · S. Turgeon · C. Sarra-Bournet · G. Laroche · D. Mantovani (✉)
Laboratory for Biomaterials and Bioengineering, Laval University, Quebec City, G1K 7P4, Canada
e-mail: Diego.Mantovani@gmn.ulaval.ca, www.lbb.gmn.ulaval.ca

Introduction

Intravascular stents are medical devices currently used to scaffold arterial lumen, most often of diseased arteries, after balloon angioplasty [1]. Introduced in the 70's, conventional balloon angioplasty, presents two major complications: abrupt vessel closure during the intervention and restenosis during follow-up [2]. Compared to angioplasty alone, stenting procedures improve the safety and efficacy of the intervention, especially by avoiding the abrupt vessel closure. However, restenosis remains the principal cause of clinical complications even after stenting procedures, leading to up to 30% of failure after 3 months of implantation [3]. Other common complications frequently observed remain thrombosis, inflammation and corrosion of the metallic stent material [4]. This latter induced by the blood fluid, causes a degradation of the mechanical properties of the metallic devices [4], thus presenting a high potential for the release of potentially toxic metallic compounds, such as nickel-based oxides and metal ions [5]. This is of particular concern because currently, the materials mainly used to fabricate metallic endovascular prostheses are 316L stainless steel and shape memory alloys, such as nickel–titanium alloys, both containing a high concentration of nickel (respectively 8 to 12% and around 50%). Animal studies show that these potentially toxic compounds are stocked in the tissues surrounding the stent and can migrate through the blood flow, to be accumulated in vital organs like kidneys, spleen and liver [6, 7]. More-

over, the effect of different concentrations of corrosion products on the growth of rat aortic cultured smooth muscle cells was studied by Shih et al. [8]. They showed that the corrosion products induced cell morphology changes and even cell necrosis. Also, the growth inhibition was correlated with the increase of nickel concentration in the corrosion products. The interactions between the metallic devices and the living tissues (including blood and arteries) occurring at their interface, the surface properties of the metallic devices play a key role in their long-term safe implantation. Therefore, one obvious approach to reduce the metallic ion release is the surface modification of the presently commercial metallic devices.

Surface modifications are a general concept that can be divided into surface treatments and surface coatings, or a combination of both. Surface treatments include mechanical and electrochemical polishing, ultrasonic cleaning, chemical etching and degreasing, as well as low pressure plasma etching [9], while surface coatings [10, 11] could be obtained by wet processes, such as dip coating, or dry processes, such as low pressure plasma deposition [12]. Moreover, it is well documented that the chemical structure of the thin film [13], as well as the adhesion properties between a coating and a metallic substrate [14], largely depend on the surface composition and morphology of the metallic substrate prior to the film deposition. Air-exposed stainless steel is naturally covered by an oxide layer (typically 10–50 Å thick) composed of metallic oxides (mainly chromium oxide Cr_2O_3) and of hydroxides. A layer of adsorbed hydrocarbons is also generally present on top of the oxide [15]. For the proper coating of a stainless steel surface, it appears clearly from the literature that three main points have to be highlighted. Firstly, it is necessary to perform the coating on a contamination-free metallic surface. Indeed, the best adhesion properties between the coating and the metallic substrate are reached when the metallic surface is clean [16,17]. Secondly, the surface roughness has to be small compared to the film thickness for the deposition to proceed correctly, for the film to be uniform and for the adhesion properties at the interface to be maximized. Finally, the oxide layer is a critical interface between the metallic biomaterial and the coating. Indeed, from a mechanical point of view, the oxide layer can be considered as a ceramic material which may therefore present a brittle behavior under stress conditions. During the stent deployment in the artery, the plastic deformation of the metallic biomaterial stresses the surface oxide, causing cracking and delamination and therefore, leading to the delamination of the coating. Moreover, it is known that oxide layers on metallic surfaces are not thermodynamically stable upon exposure to biological environments [18]. On these bases, it appeared that the complete removal of the oxide layer was one of the key tasks prior to any further coating development. The general objective of this work was therefore to develop and optimize a specific pre-treatment process for AISI 316 stainless steel to prepare its surface for further plasma-deposited polymer coating for biomedical applications.

Among the known surface pre-treatments of stainless steel, electrochemical polishing was considered in this study because it presents the following advantages: 1) it can indeed be performed on complex sample shapes, such as endovascular stents, leading to smooth, defect-free and contamination-free surfaces; 2) it allows the removal of non-metallic inclusions and irregularities related to initialization of the corrosion processes [19, 20], especially local corrosion [21]. Although the mechanisms governing the electropolishing are not yet fully understood, they are generally explained by two different reactions at the anode surface [22, 23]. The formation of a thick, viscous diffusion layer, at the liquid-solid interface, controls smoothing of the surface, by the dissolution of peaks having dimensions greater than 1 micron (macro smoothing). The formation of a thin solid film on the surface controls brightening by dissolution of peaks down to 0.01 micron (micro smoothing). By this anodic dissolution process, the original oxide layer is removed and a new one is formed which is thinner, cleaner and chemically more homogeneous. Indeed, two reactions are in competition at the same time during the electropolishing process: The dissolution of metallic elements (such as Fe as Fe(II)) through a prepassive layer featuring a reaction with free water, and the passivation process depicted as a solid-state formation of oxidized metallic elements (such as Fe(III)). Bojinov et al. showed clearly that the electropolishing of iron in concentrated phosphoric acid leads to the formation of a layer of passivating species which progressively blocks the prepassive dissolution of the metal [24].

The main objective behind this work was the encapsulation of the metallic devices by a thin film of plasma-polymerized fluorocarbon which would act as a barrier against ion release while being biocompatible, stable for long-term implantation, impermeable (even after stent deployment), cohesive and well-adherent to the metallic substrate. An electropolishing process was developed because the chemical structure of the thin film and the adhesion properties between the coating and the metallic substrate largely depend on the surface composition and morphology of the metallic substrate prior to the film deposition. Smoothing phenomena, as well as changes in the chemical composition of the electropolished surface, are controlled by numerous parameters such as the current density, the temperature and the composition of the electrolyte, the bath configuration and the duration of the treatment [23, 25, 26]. Thus, the specific aim of this work was to optimize the experimental conditions of the electropolishing process of laminated 316 stainless steel sheets. For each tested set of conditions, the effects of electropolishing process on topography, roughness and chemical composition of AISI 316

stainless steel surface were investigated by Atomic Force Microscopy (AFM), Scanning Electron Microscopy (SEM) and X-ray Photoelectron Spectroscopy (XPS). First, the usefulness of an acidic dipping post-treatment was demonstrated. It was indeed shown that acidic dipping was necessary to remove the phosphate layer inevitably formed by the electrochemical process. Then, the optimal conditions of electropolishing were determined, in terms of reduction of the oxide and contamination thickness and in terms of reduction of the surface roughness and of the density of defects. Finally, three different surface finishes were electropolished under optimal conditions, and the final surface mean roughness was evaluated.

Materials and methods

Materials

Flat 316 stainless steel (Quebec Metal Pressing Inc., Montréal, Canada) specimens (15 × 10 × 1.5 mm) were used as metallic substrates. Their composition is as follow (wt. %): Cr (16.00–18.00), Ni (10.00–14.00), Mo (2.00–3.00), Mn (≤ 2.00), Si (≤ 1.00), C (≤ 0.08), P (≤ 0.045), S (≤ 0.03) and Fe (balance). Some specimens were used as received from the manufacturer in their laminated form, others were mechanically polished to a finish # 4, according to metallurgical standards and some were polished to a mirror like finish, with successive grits down to a final 0.1 μm diamond powder. Prior to the electropolishing process, the specimens were cleaned successively in acetone, deionized water (D.I.), and isopropanol for 10 minutes each in an ultrasonic bath, and subsequently dried with particle-free compressed air.

Surface treatments

Electrochemical polishing

A glass container was used as the electrolytic polishing cell (115 mm long, 100 mm wide and 80 mm high). The sample was used as the anode (positive potential) and a 316 stainless steel sheet with the same dimensions was used as the cathode (negative potential). The distance between the two electrodes was fixed at 60 mm. The current density was fixed at 0.75 A.cm^{-1} and the immerged surface of each electrode at 2 cm^2 [27, 28]. The electrolyte was composed of a mixture typical for electropolishing [23], but optimized for stent applications by De Scheerder *et al.* [27, 28]: glycerol at 99+% (50% v/v), phosphoric acid at 85% (35% v/v), and D.I. water (15% v/v). Glycerol and phosphoric acid were purchased from Laboratoire MAT (Montréal, Canada). For each treatment, a new fresh electrolyte was used, because it is known that modifications of the metallic ion concentration could have an influence on electropolishing conditions [29]. The volume of electrolyte was 100 ml and the pH before electropolishing was 5. The required duration of the process and the temperature of the electrolyte were optimized experimentally, in order to reach the lowest value in terms of roughness, contamination and oxide layer thickness.

Acidic dipping

The dipping in the acidic solution (which had been optimized previously) was performed by immersion of the metallic sample in a mixture of nitric acid at 70% (10% v/v), hydrofluoric acid at 50% (2% v/v) and D. I. water (88% v/v), during 30 s at 50°C. Nitric acid and hydrofluoric acid were purchased from Laboratoire MAT and BDH, respectively (both in Montréal, Canada). Then, the samples were thoroughly rinsed with D.I. water and dried with particle-free compressed air after each dipping.

Surface analysis

Topographic evaluation and roughness measurements

Atomic Force Microscopy (AFM) investigations were performed using the tapping mode of a Dimension^{TM} 3100 Atomic Force Microscope (Digital Instrument, CA, USA) with an etched silicon tip (OTESPA^{TM}). Surface roughness was evaluated at two different scales, using the classical mean surface roughness parameter R_a, calculated at two scales: over an area of 20 × 20 μm and an area of 80 × 80 μm. Eight areas per treatment were tested for R_a calculations over 20 × 20 μm and six over 80 × 80 μm. R_a was defined by the usual expression:

$$R_a = \frac{1}{LxLy} \int_0^{Lx} \int_0^{Ly} \left| f_{x,y} \right| dxdy$$

where R_a is the mean value of the surface relative to the center plane, f (x, y) is the surface relative to the center plane, and L_x L_y are the dimensions of the scanned surface. In our study, L_x and L_y were equal and set to 20 μm or 80 μm. Stylus prfilometry measurements were also performed using a Dektak 3, in order to get information about the surface roughness at a macroscopic scale. R_a was calculated over a 1 mm line, and six lines were tested per surface treatment. R_a was defined by the same expression as above, but applied in 1 dimension. Scanning Electron Microscopy (SEM) imaging

was performed on a JEOL JMS-35CF (15 KeV, X 1200 and X 600), in order to evaluate the effect of the process on the surface topography.

Chemical composition

The chemical composition of the surface was investigated by an X-Ray Photoelectron Spectrometer (XPS–PHI 5600-ci spectrometer–Physical Electronics), with a base pressure below 5×10^{-9} mbar. Surveys and depth profiles were acquired at low resolution, using the K_a line of a standard aluminium X-Ray source powered at 400 W. Survey spectra were recorded at a detection angle of 45° with respect to the surface plane. Sputtering for depth analyses was performed with a beam of Ar^+ ions of 4 KeV energy and 0.6 μA/cm^2 current density, at an incident angle of 45° over a surface of ~0.2 cm^2. As the stochiometry of the oxide layer is variable, the oxide layer thickness will be arbitrarily defined as the point where the oxygen signal decreases to half-maximum [9].

Results and discussion

Acidic dipping

Figure 1 shows SEM micrographs of three surfaces of stainless steel with the corresponding surface chemical composition obtained by XPS: one as-received surface of stainless steel without treatment (Fig. 1.a.), one electropolished (for 5 min. at room temperature) surface (Fig. 1.b) and one electropolished (for 5 min. at room temperature) surface subsequently acid dipped (Fig. 1.c).

A clear contrast in surface topographies can be easily observed in Fig. 1. The as-received surface (Fig. 1.a.) shows the typical microstructure of a laminated surface of stainless steel, with deep fissures and scratches. The material is covered by a porous oxide layer [30, 31] that is rich in

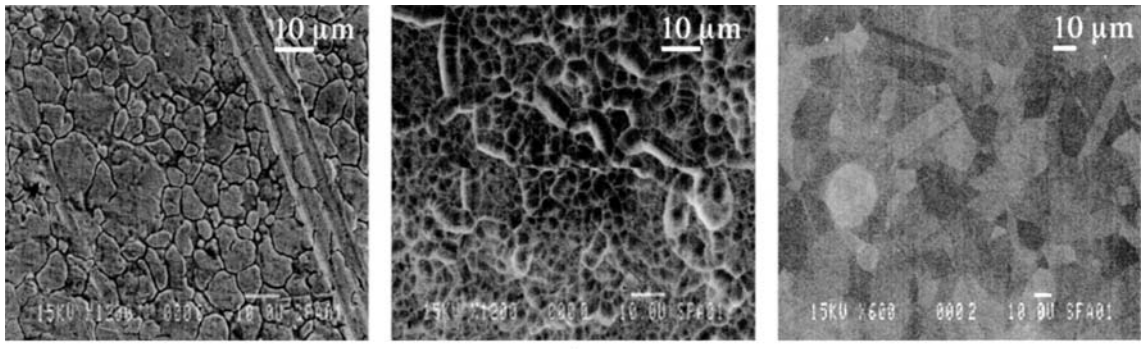

Elements	At. (%)		
	a	b	c
C	42.3	20.4	18.3
O	**42.8**	**61**	**54.1**
Fe	4.4	5.5	8.4
Cr	5.8	3.6	12.8
Mo	-	-	0.2
Ni	0.5	-	2
P	-	**9**	**1.4**
F	0.8	-	1.8
N	2.5	0.5	1
Others	0.9	-	-

Fig. 1 SEM micrographs and XPS survey data (Atomic %)–316 stainless steel surfaces; (a) as-received; (b) electropolished; (c) electropolished and acid dipped.

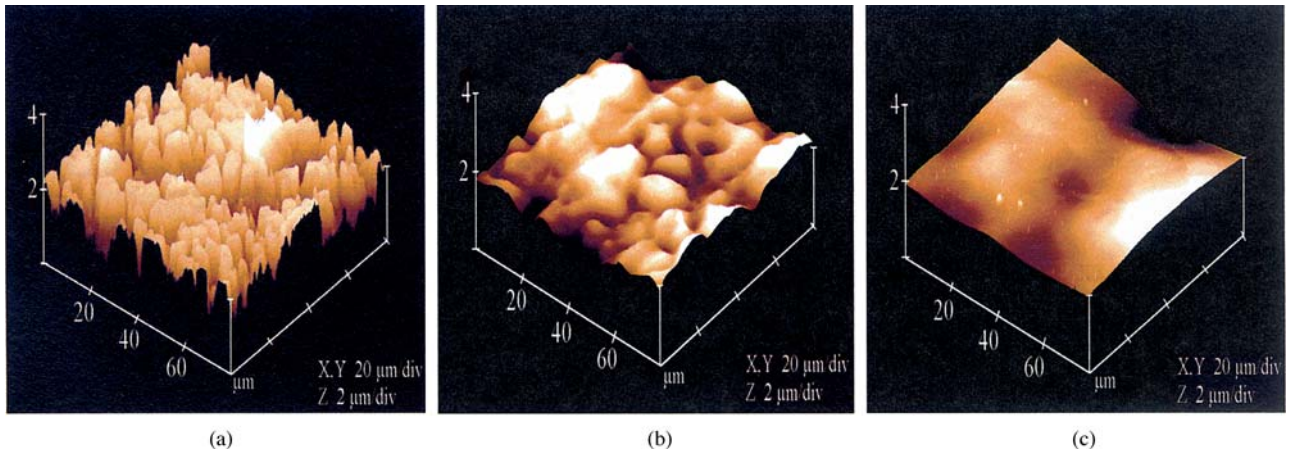

Fig. 2 AFM micrographs–316 stainless steel surfaces; (a) as-received; (b) electropolished for 1.5 min at room temperature; (c) electropolished for 5 min at room temperature.

carbon (42.3 at.%), and oxygen (42.8 at.%), and presents some traces of contaminants like nitrogen and fluorine. On the electropolished surface (Fig. 1.b.), a singular surface appears, characterized by randomly distributed hemicylindrical features. According to the XPS data, the electropolished surface is composed of phosphates as well as oxides with some remaining organic contaminants. Indeed, the phosphate layer obtained could originate from the anodic film responsible for the macro smoothing. A yellow film covering the implants has been already observed after electropolishing stainless steel implants in a sulphuric-orthophosphoric electrolyte [32]. This film probably originated from the thick and viscous anodic film, formed at the surface of the implant during the electropolishing treatment. The acid treatment removed mostly the phosphate layer (Fig. 1.c.) and the surface appears homogeneous and smooth, and the grain boundaries, characteristic of the bulk structure can be clearly distinguished. The oxygen atomic concentration is reduced after the treatment with acid (from 61 at.% to 54.1 at.%), and this decrease is balanced by the increase of atomic concentrations of metallic compounds, mainly chromium. The atomic concentration of carbon is lowered by the acid dipping (18.3 at%), compared to the as-received substrate (42.3 at.%). The carbon contamination was reduced by the combination of electropolishing and acid dipping. Fluorine was also detected (1.8 at.%) on the surface treated by electropolishing and acid dipping, originating from the acid solution. Although some phosphorus (1.4 at.%) was still detected, we can conclude that the acid dipping is essential to remove the phosphate layer on top of the electropolished stainless steel samples and to improve the general surface quality. Therefore, the acid dipping was systematically applied after each electropolishing treatment for the optimization of the electropolishing process.

Duration of electropolishing treatment

The relationship between the composition and the topography of the metallic surface, and the duration of electropolishing, was investigated for room electrolyte temperature, at the beginning of the treatment. Indeed, an increase of the electrolyte temperature was noted during electropolishing, reaching 60°C after around 3 minutes of treatment.

Figure 2 shows 3-dimension AFM pictures of stainless steel surfaces as a function of the electropolishing duration. Fig 2.a. shows an as-received surface while Fig. 2.b. and Fig. 2.c. show surfaces that were electropolished for 1.5 minutes and 5 minutes, respectively. It appears that the longer is the duration of electropolishing, the smoother the surface becomes. Again, the as-received surface appears strongly damaged, presenting irregularities and pits more than 2 μm deep. After 1.5 minutes of electropolishing, the surface is smoother, surface irregularities are less deep ($\sim$0.5 μm). After 5 minutes of electropolishing, the surface results homogenous, smooth, defect-free, and the grain boundaries, characteristic from the bulk structure, are visible. Moreover, smooth features with hills and valleys are observed, characteristic of an electropolished surface [32]. It can be concluded that the surface becomes smoother as the duration of electropolishing increases, and this effect was also reported by Rao et al., in a mixture of orthophosphoric acid, sulphuric acid and chromic acid at room temperature [33]. We noted that the grain boundaries begin to be distinguishable after only 3 minutes of electropolishing, with smaller steps between them. Indeed, electropolishing removes materials from the substrate with a different rate for each grain, because each grain has a different crystallographic orientation. The resulting grain boundaries at the top of the surface are comparable to sharp steps that are more or less high, depending on the electropolishing process conditions.

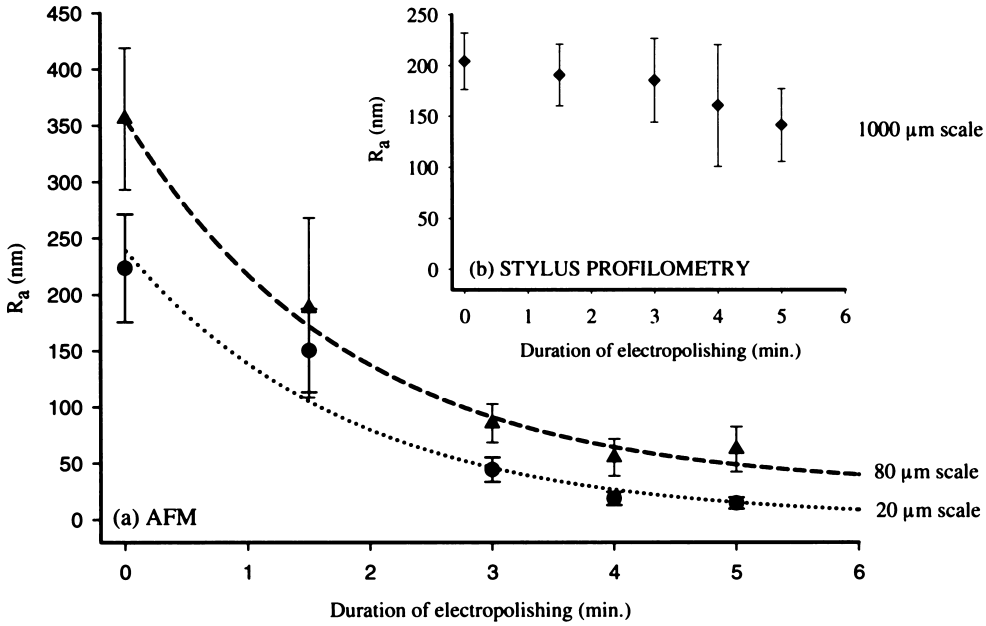

Fig. 3 Mean roughness parameter R_a, versus duration of electropolishing–316 stainless steel surfaces; (a) measured by AFM, scanned over 20 × 20 μm and 80 × 80 μm, with both fitted curves having a decay constant of 0.55 min^{-1}; (b) measured by stylus profilometry scanned over 1000 μm.

Figure 3 shows the mean roughness R_a versus the duration of electropolishing, calculated for three different scales, 400 μm^2 and 6400 μm^2 and 1 mm. The mean roughness R_a measurements presented in Fig. 3 confirm the qualitative information described in the previous paragraph. The original surface mean roughness is of the order of 220 nm, 370 nm and 210 nm for the 20 μm, 80 μm and 1000 μm scales respectively. The mean roughness R_a parameters follow the same exponential decay for the 20 μm and 80 μm scales. Only the amplitudes and final asymptotes vary. These asymptotes are some few nm for the 20 μm scale and ∼20 nm for the 80 μm scale. A similar decay was already observed by Lee et al. [34] but the exponential behavior was not pointed out. From a theoretical standpoint, the rate of smoothing was already studied for simple and complex surface profiles. In 1954, Wagner studied the rate of anodic leveling of low sinusoidal profiles, in a case of an ideal electropolishing process, and an analytical solution predicted an exponential decay of profile amplitude with dissolution time [35]. For the macroscopic scale, the mean roughness measured by stylus profilometry shows no significant evolution for the first 3 minutes of electropolishing, with R_a constant at ∼190 nm. Only a slight decrease is noted for longer times of electropolishing.

Table 1 shows XPS survey data (atomic percentage) for the as-received stainless steel surfaces and for the electropolished surfaces for 3 minutes. Since no significant effect of the duration of electropolishing on the chemical surface concentrations could be noted, only a typical electropolished surface concentration is presented. Compared to the as-received stainless steel surface, these surfaces present low concentrations of carbon and other impurities, but higher concentrations of oxygen and metals, mainly iron and chromium. The average ratio Cr/Fe is 1.62 for the electropolished surfaces, and 1.32 for the non-electropolished one. Since the effectiveness of the surface passivation is correlated with surface chromium enrichment [36], it can be concluded that the passivation ratio is higher for the electropolished surfaces than for the as-received one. So, the concentrations of oxygen and of metallic elements increase for the electropolished surfaces, if compared to the as-received surface. This can be explained by the presence of the layer of passivating species. Fluorine traces (∼1%) are also detected on the electropolished surfaces, originating from the acidic dipping in the solution containing HF, as well as phosphor traces (∼1%), originating from the process that contains phosphoric acid.

Altogether, surface topographic information, roughness measurements and surface chemical composition analyses, demonstrated that the electropolished surfaces tend to be defect-free, smooth and less contaminated than the as-received surfaces. Nevertheless, since no difference in terms

Table 1 XPS survey data (Atomic %) versus duration of electropolishing—As-received and electropolished (3 min.) 316 stainless steel surfaces.

	At.%						
Stainless steel surface	O	C	Fe	Cr	Ni	Mo	Others
As-received	42.8	43.3	4.4	5.8	0.5	–	3.2
Electropolished (3 min.)	52.3	25.6	6.6	10	1	0.1	4.4

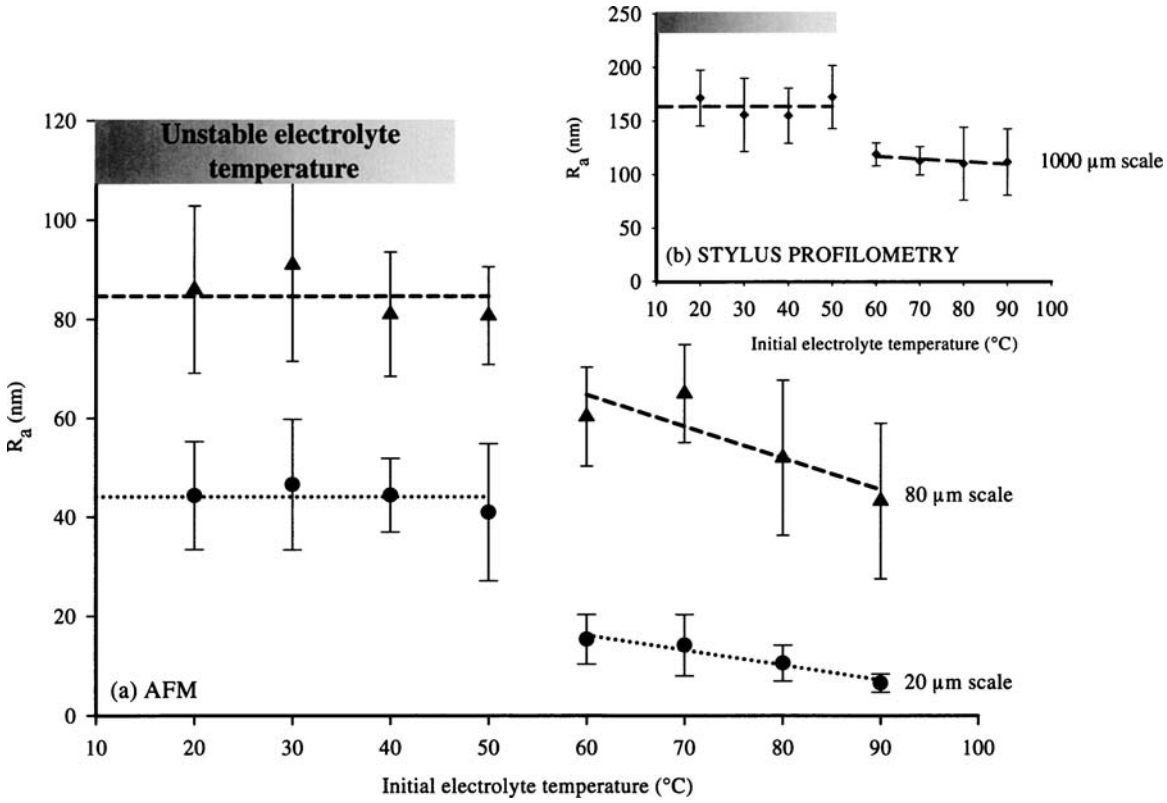

Fig. 4 Mean roughness parameter R_a, versus initial electrolyte temperature–316 stainless steel surfaces; (a) measured by AFM, scanned over 20×20 μm and 80×80 μm; (b) measured by stylus profilometry scanned over 1000 μm.

of the chemical composition was observed between the surfaces electropolished for different durations, the optimal duration of electropolishing was chosen as a function of the topography and the roughness. After 3 minutes of electropolishing, the grain boundaries begin to appear, as shown by AFM pictures (results not shown), but still constitute very small steps compared to the overall roughness which is already low ($R_a \approx 44$ nm for the 20 μm scale). Longer treatments lead to grain boundaries which are more shifted from one another, resulting in numerous large steps, offsetting the benefits of the further decrease of overall roughness. Thus, the duration of electropolishing was fixed at 3 minutes for all subsequent experiments.

Electrolyte temperature

Figure 4 shows the mean roughness parameter R_a of surfaces electropolished for 3 minutes, versus the electrolyte temperature at the beginning of the electropolishing treatment. As for the duration of electropolishing, R_a was calculated for three different scales, 20 μm, 80 μm and 1000 μm. For the three scales, two regions can be distinguished, one from room temperature to 60°C, and the other from 60°C to 90°C. It is worth noting that 60°C is the final electrolyte temperature attained before the end of every experiment made with an initial electrolyte temperature below 60°C. In the first region, where the electrolyte temperature is not stable during the electropolishing process, the mean roughness is constant around 44 nm, 85 nm, and 163 nm for 20 μm, 80 μm and 1000 μm scales, respectively. Since the electrolyte temperature is not stable during the process, no conclusion can be pointed out for this region. In the second region, where the electrolyte temperature is stable, the mean roughness decreases linearly, at the microscopic scales, when the temperature of the electrolyte is increased. Therefore, optimum electropolishing conditions are probably achieved when dissolution of the compact anodic layer on the metallic substrate is under mass transport control [22, 37], which is the dominating process at high temperatures as opposed to the kinetic steps, which are the dominating process at low temperatures [23]. Thus, this is consistent with the fact that electropolishing, and particularly macro smoothing, is more efficient at higher temperatures. At macroscopic scale, the decrease of temperature in the range where the electrolyte temperature is stable is insignificant.

Table 2 shows XPS survey data (atomic percentage) for surfaces non-electropolished and electropolished at room temperature (20°C) and above it. A slight improvement of the quality of the surface was observed for the surface electropolished at room temperature, if compared to the as-received one. Above room temperature, no significant effect of the

Table 2 XPS survey data (Atomic %) versus initial electrolyte temperature—316 stainless steel surfaces.

Stainless steel surface	At.%						
	O	C	Fe	Cr	Ni	Mo	Others
As-received	42.3	43.1	4	5.7	0.3	—	4.6
Electropolished							
T = 20°C	52.3	25.3	6.6	10	1	0.1	4.4
T > 20°C	57.5	18.7	7.2	11.5	1.3	0.2	3.6

initial electrolyte temperature on the chemical concentrations was noted.

Altogether, surface topographic information, roughness measurements and chemical surface composition analyses, demonstrated that the optimal electrolyte temperature was higher than 90°C. At 90°C, the temperature was stable during the entire electropolishing process, and the surface obtained is homogeneous, smooth, defect-free and less contaminated than the as-received surface.

In-depth analyses

Figures 5 and 6 show the XPS in-depth composition profiles, for an as-received surface, and an electropolished surface under the optimal conditions (3 minutes at 90°C). The mean roughness R_a is also indicated for the 20 μm scale. Both graphs show a similar general behavior. The oxide layer was clearly detected at the surface, while the characteristic atomic composition of the alloy is observed deeper in the sample. The main characteristic of the oxide layer is the presence of oxygen and an excess of chromium. For the as-received surface, the oxygen profile increases slightly for very short sputtering time, and then it gradually decreases without reaching zero (due to the water residual pressure in the analysis chamber and at high reactivity of the exposed metal). A similar behavior was observed for chromium: it increases first, and then slowly decreases to reach the alloy's chromium bulk concentration. For the electropolished surface, the XPS signal intensity of oxygen decreases rapidly right after the beginning of the sputtering. The thickness of the oxide layer of the electropolished surface is smaller by approximately half than that of the as-received surface. The chromium content in the oxide layer is higher for the electropolished surface than for the as-received one, while the iron content is quite the same. For both surfaces, nickel is also detected but at a low concentration in the oxide layer, and it increases slowly until it reaches the bulk concentration. The coverage by carbon is mostly confined to the topmost layer. Nevertheless, in the case of the electropolished surface, the XPS signal intensity of carbon is lower and decreases to zero faster than in the case of the as-received surface. Traces of phosphor (not shown) are only detected on the very surface of the electropolished surface, showing that it does not penetrate deep into the material during electropolishing. Finally, the mean surface roughness (scanned over 20 × 20 μm) is approximately thirty times lower for the electropolished surface than for the as-received one, as shown by the mean roughness parameter R_a on Fig. 5 and 6.

Altogether, these data demonstrate that the electropolishing process produces a smooth, defect-free surface. The

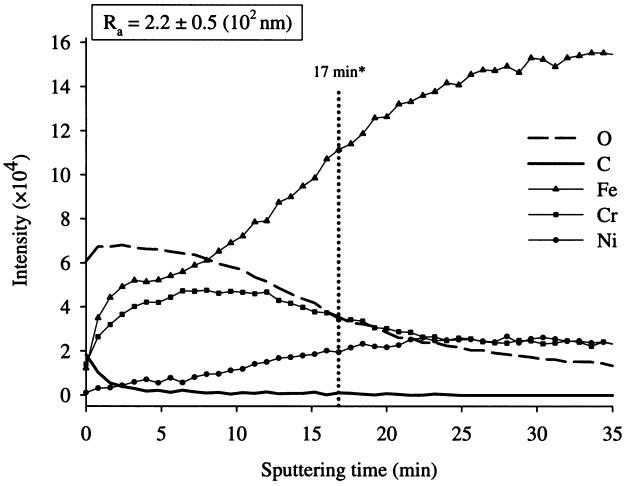

Fig. 5 XPS depth profile—As-received 316 stainless steel surface (*oxide layer thickness arbitrarily defined as the point where the oxygen signal decreases to half-maximum).

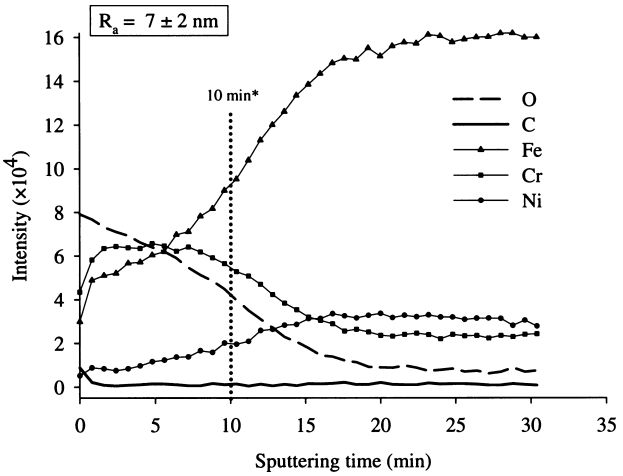

Fig. 6 XPS depth profile—Electropolished 316 stainless steel surface under optimized conditions (3 min, 90°C) (*oxide layer thickness arbitrarily defined as the point where the oxygen signal decreases to half-maximum).

Table 3 Mean roughness parameter R_a, versus initial surface finishes before and after electropolishing measured by AFM, scanned over 20 × 20 μm and 80 × 80 μm and measured by stylus profilometry scanned over 1000 μm.

	$R_a(10^2$ nm)		
	20 × 20 μm scanned	80 × 80 μm scanned	1000 μm scanned
Before electropolishing			
As-received	2.2 ± 0.5	3.7 ± 0.5	2.1 ± 0.3
Finish # 4	2.3 ± 0.2	4.1 ± 0.4	3.5 ± 0.5
Mirror-finished	0.04 ± 0.01	0.12 ± 0.02	0.30 ± 0.06
After electropolishing			
As-received	0.07 ± 0.02	0.26 ± 0.05	1.3 ± 0.4
Finish # 4	0.08 ± 0.03	0.61 ± 0.07	1.8 ± 0.4
Mirror-finished	0.05 ± 0.01	0.31 ± 0.08	0.51 ± 0.05

thickness of the oxide layer is also decreased, as well as the carbon contamination. In general, it can be concluded that the surfaces obtained by electropolishing presented all the advantages required prior to plasma etching and subsequent plasma coating.

Effects of different initial surface finishes on the final surface mean roughness

Samples, with three different surface finishes were electropolished under the optimal conditions (3 minutes at 90°C). An as-received surface and two mechanically polished surfaces (an industrial surface finish # 4 and a mirror-finished with diamond powder 0.1 μm) were also considered before and after electropolishing. Table 3 presents the results of the mean roughness for the three surface finishes, before and after electropolishing, at the three scales.

Before electropolishing, as-received and finish # 4 surfaces present a similar mean roughness, ∼220 nm at the 20 μm scale and ∼400 nm at the 80 μm scale, but at the 1000 μm scale, the mean roughness of the finish # 4 surfaces result to be higher than the one of the as-received surface. The mean roughness results to be lower for the mirror-finished surface: 4 nm at the 20 μm scale, 12 nm at the 80 μm scale and 30 nm at the 1000 μm scale. After electropolishing, as-received and finish # 4 surfaces again have a similar mean roughness, ∼8 nm over at the 20 μm scale, but at the 80 μm scale, the mean roughness of the as-received surface is less than half (R_a ∼26 nm) of the one of the finish # 4 surface (R_a ∼61 nm). After electropolishing, the mean roughness of the mirror-finished surface is 5 nm at the 20 μm scale, and thus, this is similar to the mean roughness of the same surface before electropolishing. However, a slight increase of roughness at the 80 μm and 1000 μm scales was observed, which is fortunately less critical. The mean roughness after electropolishing depends on the initial mean roughness, except for already relatively smooth ones. The electropolishing process leads to smoother surfaces in the case of initial rough surfaces (as-received and finish # 4 surfaces), but not in the case of mirror-finished surfaces. Generally, the smoother the surface is prior to electropolishing, the smoother the surface will be after it. Finally, the roughness was higher at the 80 μm and at the 1000 μm scales, than at the 20 μm scale, but tended to be more efficiently reduced for the as-received samples than for the finished number 4 samples. The fissures of the lamination-produced oxide are apparently less difficult to smoothen than the deep scratches generated by the mechanical polishing.

By only considering the effect on the mean surface roughness, it can be concluded that mechanical polishing to mirror-finished should be appropriate surface treatments, instead of electropolishing, in order to obtain the smoothest surface over any scale. Nevertheless, it was shown in a previous study that mechanical polishing leaves a surface with microscopic irregularities, which are not desirable for further polymer coating [38]. On the opposite, the mean surface roughness measured on electropolished surface results from the difference in height between relatively large hills and valleys, rather than from surface microscopic defects. This structure is characteristic of an electropolished surface [32] and the result is a very smooth, defect-free surface. Finally, electropolishing is mandatory to obtain a good surface quality, and can be used alone or in combination with mechanical polishing. In fact, mechanical polishing decreases the mean roughness on a larger scale (macro- and micro-scales), while electropolishing treatment decreases the mean roughness on a smaller scale (micro- and nano-scales).

Summary and conclusion

The aim of this study was to develop a pre-treatment for 316 stainless steel surfaces to optimize the interface properties with the subsequent plasma-deposited fluorocarbon thin film to maximize the interfacial adhesion between the substrate and the plasma-deposited thin coating, even after severe plastic deformation. Firstly, the experimental conditions of electropolishing, such as the use of acid dipping as a

post-treatment, duration of the treatment and electrolyte temperature, were optimized. Secondly, XPS in-depth composition profiles of an as-received surface and an electropolished one were performed. Results showed that the thicknesses of the oxide layer and of the carbon layer decreased after the treatment. Even if the surface oxide was not completely removed (because of the instantaneous re-oxidation of the metallic surface after air contact), it was reduced to less than half of the oxide thickness of an as-received surface. Finally, the effect of the initial surface roughness of the stainless steel samples on final electropolished surface roughness was studied. Results showed that the mean roughness after electropolishing depends on the initial mean roughness, except for already relatively smooth surfaces.

Acknowledgements The authors would like to thank Michel Fiset, professor at the Material Engineering Department at Laval University, for his help and guidance, Simon Michaud, undergraduate student, for his assistance in the electropolishing experiments, Fatiha El Feninat, post-graduate student, for developing the acid treatment and Richard Janvier for SEM analyses. This work was supported by the Natural Science and Engineering Research Council (NSERC-Canada) and *Fonds Québécois de recherches sur la Nature et les Technologies* (FQRNT-Québec). Marie Haïdopoulos is the recipient of a doctoral grant from the research Center of St-François d'Assise Hospital, in Quebec City.

References

1. T. W. DUERIG and A. R. PELTON, An overview of superelastic stent design. *Mater. Sci. Forum* **394–395** (2002) 1–8.
2. E. EECKHOUT, L. KAPPENBERGER and J.-J. GOY, Stents for intracoronary placement: current status and future directions. *JACC* **27** (4) (1996) 757–765.
3. H. WIENEKE, T. SAWITOWSKI, S. WNENDT, A. FISHER, O. DIRSCH, A. KAROUSSOS and E. R., Stent coating: a new approach in interventional cardiology. *Herz* **27** (2002) 518–526.
4. G. RIEPE, C. HEINTZ, E. KAISER, N. CHAKFE, M. MORLOCK, M. DELLING and H. IMIG. What can we learn from explanted endovscular devices? *Eur. J. Vasc. Endovascular. Surg*. **24** (2) (2002) 117–122.
5. O. F. BERTRAND, R. SIPEHIA, R. MONGRAIN, J. RODES, J. C. TARDIF, L. BILODEAU, G. COTE and M. G. BOURASSA, Biocompatibility aspects of new stent technology. *J. Amer. Coll. Cardiol. Field* **32**(3) (1998) 562–71.
6. S. A. BROWN, K. ZHANG, K. MERRITT and J. H. PAYER, In vivo transport and excretion of corrosion products from accelerated anodic corrosion of porous coated F75 alloy. *J. Biomed. Mater. Res.* **27** (1993) 1007–1017.
7. M. L. PEREIRA, A. M. ABREU, J. P. SOUSA and G. S. CARVALHO, Chromium accumulation and ultrastructural changes in the mouse liver caused by stainless steel corrosion products. *J. Mater. Sci.-Mater. Med.* **6**(9) (1995) 523–7.
8. C.-C. SHIH, C.-M. SHIH, Y.-L. CHEN, Y.-Y. SU, J.-S. SHIH, C.-F. KWOK and S.-J. LIN, Growth inhibition of cultured smooth muscle cells by corrosion products of 316 L stainless steel wire. *J. Biomed. Mater. Res.* **57** (2) (2001) 200–207.
9. S. TRIGWELL, R. D. HAYDEN, K. F. NELSON and G. SELVADURAY, Effects of Surface Treatment on the Surface Chemistry of NiTinol Alloy for Biomedical Applications. *Surf. Interface Anal.* **26** (1998) 483–489.
10. M. N. BABAPULLE and M. J. EISENBERG, Coated stents for the prevention of restenosis: Part 1. *Circulation* **106** (2002) 2734–2740.
11. M. N. BABAPULLE and M. J. EISENBERG, Coated stents for the prevention of restenosis: Part. II. *Circulation* **106** (2002) 2859–2866.
12. P. ROSSINI, P. COLPO, G. CECCONE, K. D. JANDT and F. ROSSI, Surfaces engineering of polymeric films for biomedical applications. *Mater. Sci. Eng. C* **23** (2003) 353–358.
13. M.-R. YANG, K.-S. CHEN and J.-L. HE, The interaction between blood and the surface characteristics of plasma polymerized films. *Mater. Chem. Phys.* **48** (1) (1997) 71–75.
14. MORSHED, M. M., B. P. McNAMARA, D. C. CAMERON and M. S. J. HASHMI, Effect of surface treatment on the adhesion of DLC film on 316 L stainless steel. *Surf. Coat. Technol.* **163–164** (2003) 541–545.
15. R. O. ADAMS, A review of the stainless steel surface. *J. Vac. Sci. Technol. A.* **1**(1) (1983) 12–18.
16. HASHIMOTO, M., Y. MIYAMOTO, Y. KUBO, S. TOKUMARU, N. ONO, T. TAKAHASHI and I. ITO, Surface modification of stainless steel in plasma environments. *Mater. Sci. Eng. A.* **A198** (1–2) (1995) 75–83.
17. L. DESHAYES, M. CHARBONNIER, N. S. PRAKASH, F. GAILLARD and M. ROMAND, Spectroscopic characterization of stainless-steel surfaces treated by plasma. *Surf. Interface Anal.* **21** (1994) 711–717.
18. N. ISTEPHANEOUS, Z. BAI, J.L. GILBERT, K. ROHLY, A. BELU, I. TRAUSCH and D. UNTEREKER, Oxide films on metallic biomaterials: myths, facts and opportunities. *Mater. Sci. Forum* **426–432** (2003) 3157–3164.
19. E. J. SUTOW, The influence of electropolishing on the corrosion resistance of 316L stainless steel. *J. Biomed. Mater. Res.* **14** (1980) 587–595.
20. D. JENKINSON, Stainless steel: The importance of being smooth and passive. *Corros. Mater.* **27** (6) (2002) 10–13.
21. A. NOE, P. HENRY, P. EGELEY and J.-C. MOUGEOT, Le polissage, traitement de surface des aciers inoxydables. *Corrosion* **18** (3) (1970) 169–173.
22. D. LANDOLT, Review article. Fundamental aspects of electropolishing. *Electrochim. Acta* **32** (1) (1987) 1–11.
23. S. MOHAN, D. KANAGARAJ, R. SINDHUJA, S. VIJAYALAKSHMI and N.G. RENGANATHAN, Electropolishing of stainless steel—A review. *Trans IMF* **79** (4) (2001) 140–142.
24. M. BOJINOV, I. BETOVA, G. FABRICIUS, T. LAITINEN and R. RAICHEFF, Passivation mechanism of iron in concentrated phosphoric acid. *J. Electroanal. Chem.* **475** (1999) 58–65.
25. W. J. M. TEGART, Facteurs susceptibles de modifier les conditions de polissage, in Polissage électrolytique et chimique des métaux au laboratoire et dans l'industrie. Dunod: Paris. (1960) 32–36.
26. P. STEFANOV, D. STOYCHEV, M. STOYCHEV, A. R. GONZALEZ-ELIPE and T. MARINOVA, XPS, SEM and TEM Characterization of Stainless-Steel 316L Surfaces after Electrochemical Etching and Oxidizing. *Surf. Interface Anal.* **28** (1999) 106–110.
27. DE SCHEERDER, I., E. VERBEKEN and J. VAN HUMBEECK, Metallic surface modification. *Semin. Interven. Cardiol.* **3** (1998) 139–144.
28. H. ZHAO, J. VAN HUMBEECK, J. SOHIER and I. DE SCHEERDER, Electrochemical polishing of 316L stainless steel

slotted tube coronary stents. *J. Mater. Sci.-Mater. Med.* **13** (2002) 911–916.
29. J. P. CAIRE, E. CHAINET, B. NGUYEN and P. VALENTI. Study of a new stainless steel electropolishing process, in AESF Annual Technical Conference. (1993).
30. D. BHASAVANICH and E.M. WILLIAMS, The influence of pre-vacuum surface conditioning on the response with electron stimulated desorption at stainless steel surfaces in uhv. *Vacuum* **30** (2) (1979) 91–92.
31. N. YOSHIMURA, T. SATO, S. ADACHI and T. KANAZAWA, Outgassing characteristics and microstructure of an electropolished stainless steel surface. *J. Vac. Sci. Technol. A* **8** (2) (1990) 924–929.
32. C. C. IRVING, Electropolishing stainless steel implants. *ASTM Special Tech. Publ.* 1985. **859**: p. 136–143.
33. T. V. RAO, R. W. VOOK, W. MEYER and A. JOSHI, Effect of surface treatments on near surface composition of 316 nuclear grade stainless steel. *J. Vac. Sci. Technol. A* **4** (3) (1986) 1604–7.
34. E.-S. LEE, Machining characteristics of the electropolishing of stainless steel (STS316L). *Int. J. Adv. Manuf. Technol.* **16** (2000) 591–599.
35. C. WAGNER, Contribution of the theory of electropolishing. *J. Electrochem. Soc.* **101** (1954) 225–228.
36. K. ROHLY, N. ISTEPHANEOUS, A. BELU, D. UNTEREKER, M. COSCIO, J. HEFFELFINGER, R. THOMAS, J. ALLEN, R. FRANCIS, A. ROBINSON, N. PERRON, B. SAHLI and B. KOBIELUSH, Effect of time, temperature and solution composition on the passivation of 316L stainless steel for biomedical applications. *Mater. Sci. Forum* **426–432** (2003) 3017–3022.
37. L. PONTO, M. DATTA and D. LANDOLT, Electropolishing of iron-chromium alloys in phosphoric acid-sulphuric acid electrolytes. *Surf. Coat. Technol.* **30** (1987) 265–276.
38. M. HAÏDOPOULOS, F. EL FENINAT, S. TURGEON, G. LAROCHE and D. MANTOVANI. Surface modification of the 316L stainless steel for the improvement of its surface biocompatibility with an RF-plasma deposited fluorocarbon coating. in the Proceeding of "ASM Conference on Materials and Processes for Medical Devices", Anaheim, CA, USA, (2003).